

See discussions, stats, and author profiles for this publication at: <https://www.researchgate.net/publication/234840409>

Terahertz Bandwidth All-Optical Modulation and Logic Using Multiexcitons in Semiconductor Nanocrystals

ARTICLE *in* NANO LETTERS · JANUARY 2013

Impact Factor: 13.59 · DOI: 10.1021/nl3044053

CITATIONS

6

READS

40

4 AUTHORS, INCLUDING:



Jonathan I Saari

ETH Zurich

13 PUBLICATIONS 157 CITATIONS

[SEE PROFILE](#)



Brenna Walsh

McGill University

15 PUBLICATIONS 102 CITATIONS

[SEE PROFILE](#)



Patanjali Kambhampati

McGill University

61 PUBLICATIONS 3,107 CITATIONS

[SEE PROFILE](#)

Terahertz Bandwidth All-Optical Modulation and Logic Using Multiexcitons in Semiconductor Nanocrystals

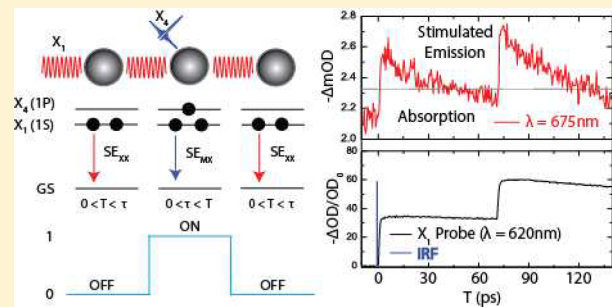
Jonathan I. Saari, Michael M. Krause, Brenna R. Walsh, and Patanjali Kambhampati*

Department of Chemistry, McGill University, Montreal, QC, H3A 2K6, Canada

Supporting Information

ABSTRACT: Optical pumping of semiconductor nanocrystals with femtosecond pulse sequences was performed in order to modulate multiexciton populations. We show for the first time that control of multiexciton populations produces high speed modulation of stimulated emission. Upon the basis of the speed of multiexcitonic processes in nanocrystals, we show modulation rates approaching 1 THz by virtue of strong quantum confinement effects. Employing femtosecond optical pulse sequences, we demonstrate all-optical logic using these nanocrystals in two forms: an AND gate, and an inverter, a key step toward all optical signal processing.

KEYWORDS: Optical logic, nanocrystals, multiexcitons, optical gain, switching, optical modulation



An increasing demand on existing communication infrastructure drives movement toward all-optical signal processing.¹ The unique size-dependent electronic structure, rich materials variability, and good chemical processability of semiconductor nanocrystals (NC) have demonstrated their promise and impact in a variety of optoelectronic applications spanning photovoltaics,^{2,3} lasers,^{4,5} photodetectors,⁶ and for LEDs.⁷ Many of these same characteristics suggest their promise as a new enabling platform for all-optical modulators, switches, and ultimately a step toward optical logic gates. In contrast to their enormous impact upon a wide variety of applications, semiconductor nanocrystals have yet to demonstrate their impact upon the realization of novel platforms for all-optical switching and logic.

Owing to strong carrier confinement, NC have a unique electronic structure that arises from excitons.^{8–12} This electronic structure has several characteristics that are advantageous for optoelectronic applications. Their transitions are tunable from the visible to the technologically relevant mid-infrared both by particle size as well as composition.¹² These transitions are moreover intense and narrow, thereby facilitating efficient optical pumping.^{4,5,13,14} A key characteristic of these NC is the degeneracies of the lower excitonic state. These NC can absorb multiple photons thereby creating multiexcitons (MX) by an Aufbau like filling of the excitonic levels.^{8,15}

Multieexcitons in NC have been well investigated due to their role in nanocrystal lasing.^{4,5,8,10,13,14} The key point toward nanocrystal lasing is that a minimal model of optical gain suggests it proceeds via stimulated emission (SE) from biexcitons (XX).^{5,8,13,14} We have recently shown that populating higher MX results in a qualitatively unique effect of gain control.^{8,13,14} Specifically, we found that higher MX

recombine at new wavelengths^{8–10,16–18} thereby resulting in the capacity to control the optical gain spectrum by prescribing specific MX states.^{8,13,14}

In existing applications which utilize MX in NC such as lasing and photovoltaics, the main constraint is the short lifetime of these states. Pioneering work by Klimov and Bawendi first showed that the multiexciton recombination (MER) rates were ultrafast, size dependent, and quantized based upon the MX multiplicity.¹⁵ For typical NC sizes and compositions, one finds $\tau_{XX} \sim 50$ ps, $\tau_{XXX} \sim 20$ ps, $\tau_{4X} \sim 5$ ps.⁶⁰ This situation poses a problem in that the optical gain lifetime is now too fast as to be useful. Hence the prevailing view of multiexcitons in nanocrystals is that they are too short-lived as to be useful in optoelectronic applications.⁶⁴

In this Letter, we show that by modulating the multiplicity of multiexcitons using femtosecond laser pulse sequences, semiconductor nanocrystals may be used as a material platform for optical switching, enabled by the physics of confinement-induced multiexcitonic interactions. These experiments reveal that two key aspects of multiexcitons in nanocrystals facilitate these operations: fast recombination rates and large interaction strengths due to strong quantum confinement effects. In addition to the first demonstration of multiexcitons as an enabling process for modulation and switching, these experiments reveal a previously unconsidered area of impact for semiconductor nanocrystals as a materials platform.⁷⁶

We perform excitonic state-resolved^{8,9} femtosecond pump/probe spectroscopic experiments, the details of which were previously described along with materials characterization

Received: November 29, 2012

Revised: January 14, 2013

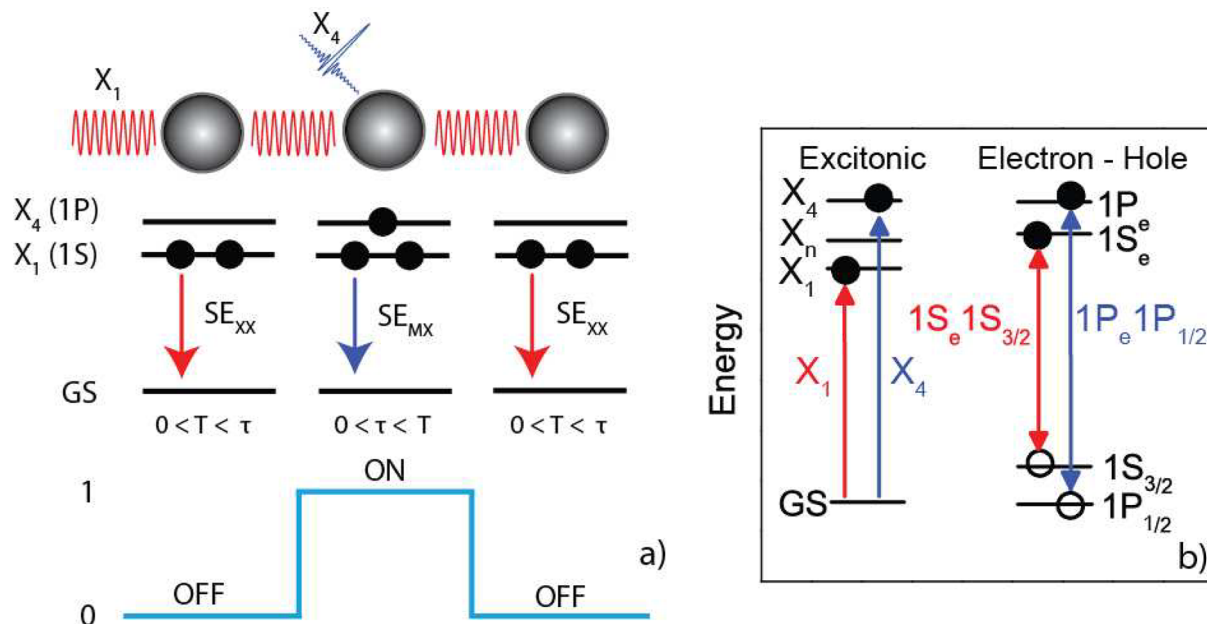


Figure 1. (a) Schematic illustration of modulating stimulated emission via multiexcitons in semiconductor NC. (b) The level structure of excitons in NC in the exciton and the electron/hole representation.

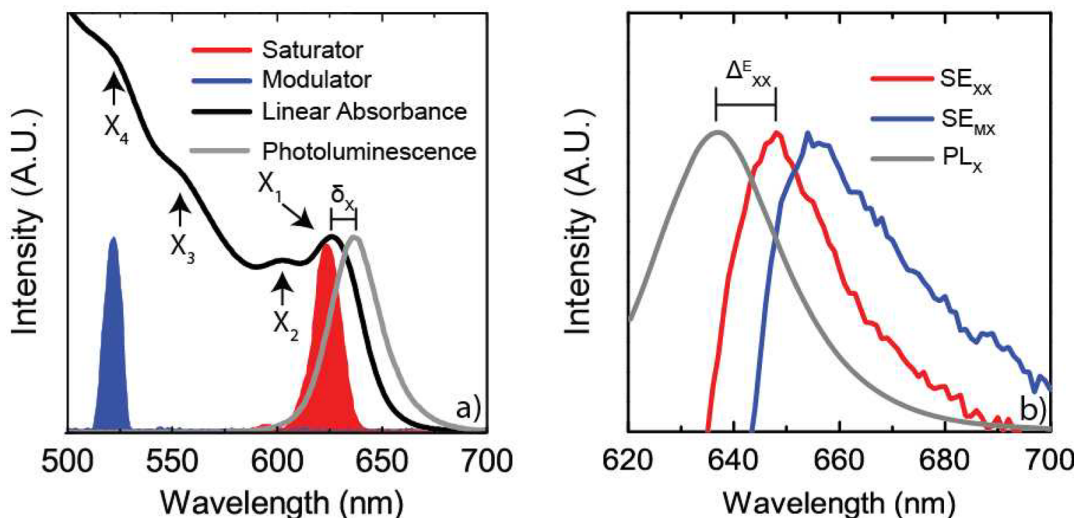


Figure 2. (a) Linear absorption and PL spectra of CdSe/ZnS NC, $R = 2.8$ nm. Shown are the excitonic transitions and the exciton Stokes shift, δ_x . (b) PL and SE spectra. The PL arises from X , whereas the SE upon pumping into X_1 (S-Type) arises from XX and the SE from X_4 (P-type) pumping arises from higher MX. Indicated is the biexciton binding energy for emissive transitions, Δ_{XX}^E . The SE spectra were obtained at $t = 2$ ps.

details.^{13,14,16,19–22} Typical instrument response functions (IRF) were ~100 fs. The CdSe/ZnS NC samples were used as received (NN-Laboratories), dispersed in toluene, and flowed at 300 K. Additional details on experimental methods and analysis are in the Supporting Information.

In order to achieve all optical modulation, we employ the following two energetically and temporally separated pump pulses: a “saturator” pulse to initialize the system for stimulated emission from biexcitons^{8,13,14} and a “modulator” pulse that creates the signal from higher multiexcitons^{8,13,14,16} to be subsequently read out, Figure 1a. Tuning the saturator resonant to the band-edge exciton (X_1) yields a nominally 1S-type exciton, whereas the modulator pulse pumps X_4 , yielding a nominally 1P type exciton,²³ Figure 1b. The CdSe/ZnS linear absorption spectrum (OD_0), photoluminescence (PL), relevant

excitonic states and corresponding pump spectra are shown in Figure 2a.

Figure 2b shows the stimulated emission (SE) spectra upon pumping into X_1 and X_4 with high fluence. The SE spectra correspond to the negative portion of the nonlinear absorption spectra, $OD_{NL} = OD_0 + \Delta OD$. The SE spectra here were obtained at a time delay of 2 ps with fluences $\sim 5 \times 10^{14}$ photons/cm². The broadening and redshifting of the SE spectra with hot exciton (X_4) pumping is consistent with our prior works.^{8,13,14} We have previously shown that this effect arises from the interaction of multiexcitons,^{8,13,14,16} and forms the basis of the switching approach used here. Specifically, higher multiexcitons emit at different wavelengths. Hence, modulating the multiplicity of the multiexciton should result in modulation of the SE signal at these red-most wavelengths.

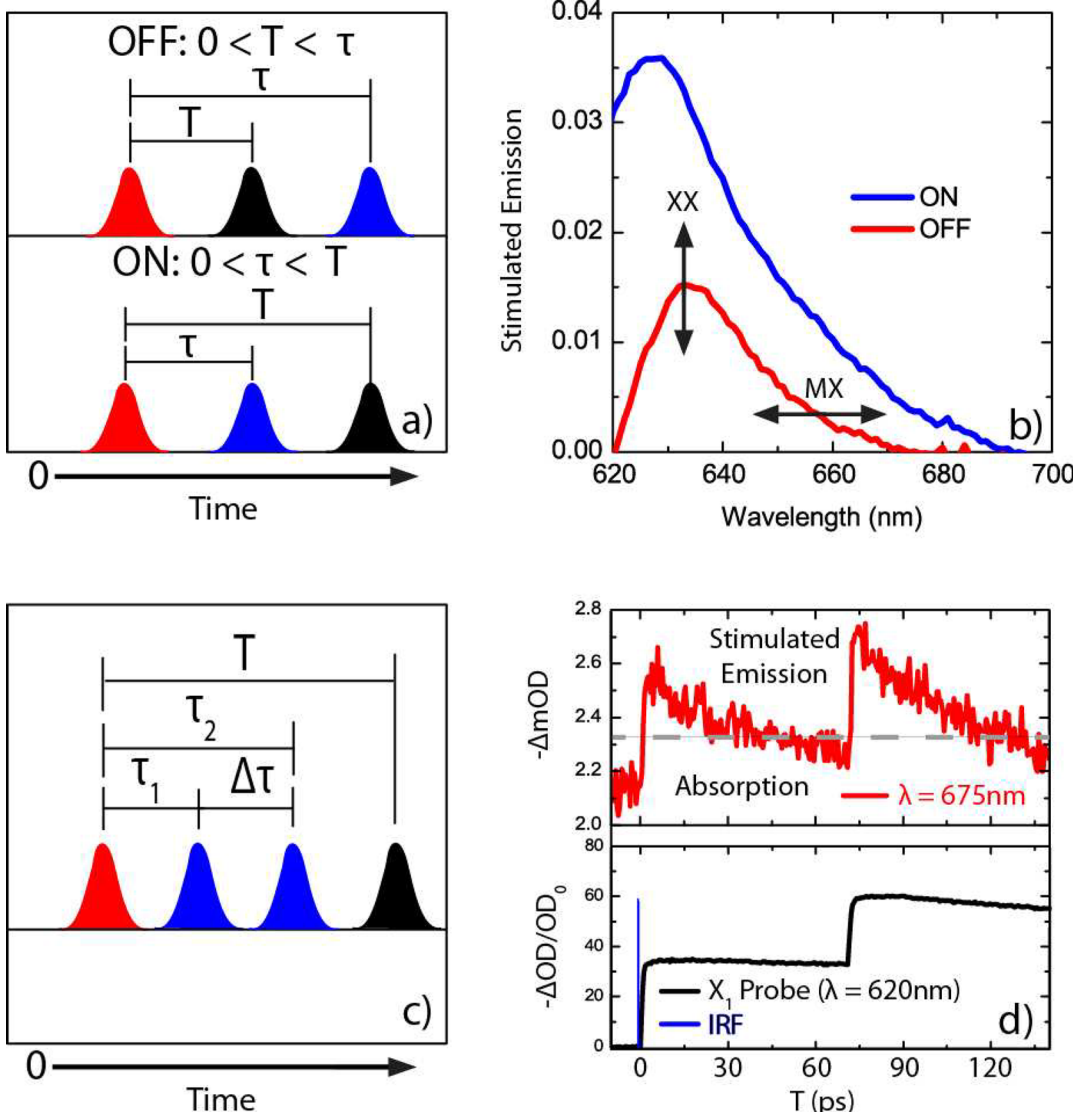


Figure 3. (a) Pumping scheme for optical modulation using saturator (X_1 pump), modulator (X_4 pump), and readout (probe) pulses depicted in red, blue, and black, respectively. T represents time difference between saturator and readout, and τ represents time difference between saturator and modulator. (b) SE spectra arising from ON/OFF pulse sequences depicted. OFF SE spectra is a result of solely pumping X_1 whereas the ON SE spectra represents contributions from modulator and saturator. (c) A modulation scheme illustrating two ON bits. (d) Experimental realization of two ON bits at a 13 GHz modulation frequency. SE transient (red trace, $\lambda_{\text{probe}} = 675\text{ nm}$) showing 75 ps peak-to-peak separation for ~ 13 GHz modulation rate. Modulator arrival times were verified *in situ* by monitoring the band edge bleaching of the X_1 transition (black trace, $\lambda_{\text{probe}} = 620\text{ nm}$).

In order to physically realize stimulated emission modulation via control of multiexciton populations, we define the time ordering of the saturator/modulator/readout pulses, Figure 3a. The time between saturator and modulator pulses, τ , has a positive value if the saturation pulse arrives at the sample before the modulator pulse. The time between the saturator and the readout (or probe pulse), T , is positive when the saturator arrives at the sample prior to the probe. The idea behind the pulse sequences is that the saturator pulse creates a XX thereby saturating the band edge exciton. The modulator adds population by pumping into the unfilled X_4 state. Hence the modulator creates MX of higher multiplicity. The two time orderings are such that the OFF state, or the purely XX state, is created when only the saturating pulse arrives prior to readout ($\tau > T$). The ON state, or MX state, is defined by both the

saturator and modulator pulses arriving prior to readout in succession ($\tau < T$). 125
126

With this time ordering, we obtain the modulation signal as well as its contrast. Figure 3b reveals that these pulse sequences produce SE signals consistent with XX or higher MX created by a single pulse. The SE from the OFF pulse sequence is identical to the SE_{XX} from a single high fluence X_1 pump. The SE from the ON pulse sequence is nearly identical to the SE_{MX} from a single high fluence X_4 pump along with a contribution from the saturator pulse. The difference between the ON and OFF states enables amplitude modulation of the SE signal as illustrated by the amplitude at 630 nm. Here, the SE_{XX} is being modulated with poor contrast. Because of gain bandwidth control from higher multiexcitons,^{8,13,14} the modulation effect is most pronounced at the red edge of the SE spectra. Near 670 nm, the modulation contrast ratio is greatly improved. 127
128
129
130
131
132
133
134
135
136
137
138
139
140

In order to directly determine modulation rates and depths, the readout is spectrally tuned to a wavelength with high contrast between ON and OFF ($\lambda = 675$ nm), while a double modulator sequence is applied, Figure 3c. Figure 3d shows experimental realization of this modulation scheme. The arrival time of the X_4 modulator pulses is measured in situ by probing the band edge exciton bleaching signal (B_1). This B_1 signal has been discussed in detail elsewhere.^{8,9,20,24} It has some amplitude of instrument response limited rise time^{20,24} thereby providing in situ timing of the modulator pulses. The X_1 30% fractional bleach ($\Delta\text{OD}/\text{OD}_0$) per modulator pulse is proportional to the number of carriers excited by the modulator pump and is consistent with $\langle N \rangle/\text{pulse} \sim 0.6$. The modulated signal is read out at 675 nm due to minimal overlapping signal from SE_{XX} . Figure 3d. From these data it is clear that the ON state is synchronized with the modulator pump. With this double pumping scheme of modulators separated by 75 ps, we demonstrate modulation with 13 GHz bandwidth at a modulation depth of >20 dB.

By modulating an intermediary pulse, we have shown that stimulated emission from multiexcitons can form a switching signal. In this case, the switch corresponds to the multiexciton multiplicity of the NC. In order to evaluate if this switching phenomenon can form a Boolean logic gate we correlate the dual binary input states with the single SE output, Figure 4.

Shown is a bit pattern with the inputs corresponding to X_1 and X_4 pumps and an output of SE_{MX} . Figure 4a. The SE_{MX} wavelength was chosen for the point of high contrast at 675 nm. By sweeping the modulator pulse from $\tau = 4$ ps to -4 ps with the saturator pulse at $T = 6$ ps, we demonstrate an inverter switch via time encoding, analogous to voltage encoding in electronic inverters. Notably, this inverter switch responds on a subpicoseconds time scale due to the relaxation time of hot excitons in NC.^{8,9,20,24} The sharp response time produces insensitivity to timing jitter of the input signals.

To demonstrate AND logic, the dual inputs were optically chopped according to the logic table depicted in Figure 4b. Stimulated emission is denoted by a positive value for $-\text{mOD}_{\text{NL}} > 0$. These spectra reveal that any single input, be it saturator or modulator, yields a 0 (OFF) output. Only the presence of dual inputs yields a 1 (ON) output, thereby showing realization of an all-optical AND gate.

We characterize the origin of the bandwidth and contrast for this optical switch in Figures 5 and 6. The switch itself acts as an amplitude modulator by virtue of modulating the amplitude of the SE at some readout wavelength. With the presence of multiple excitonic states there exists the possibility of additional channels in a wavelength division multiplexing scheme. Figure 5a shows the SE signal as a function of the amplitude of the modulator pulse. The normalized SE spectra reveal the presence of additional SE bandwidth at the red that may be used to generate additional modulation channels. Amplitude modulation of SE_{XX} at 635 nm shows a sublinear fluence dependence (inset) due to saturation of X_1 with $N = 2$. The linear fluence dependence for SE_{MX} amplitude at 675 nm is consistent with a primarily SE_{XXX} signal: increasing modulator fluence increases XXX population without saturating. From these saturation curves, one finds that higher pulse energies enable faster modulation speeds and higher contrast.

The contrast of the switch arises from the overlap of the multiexcitonic signals, Figure 5b. We model the ON and OFF SE switching states based upon our prior works on optical gain bandwidth control.^{13,14,16} A Poisson distribution of higher MX

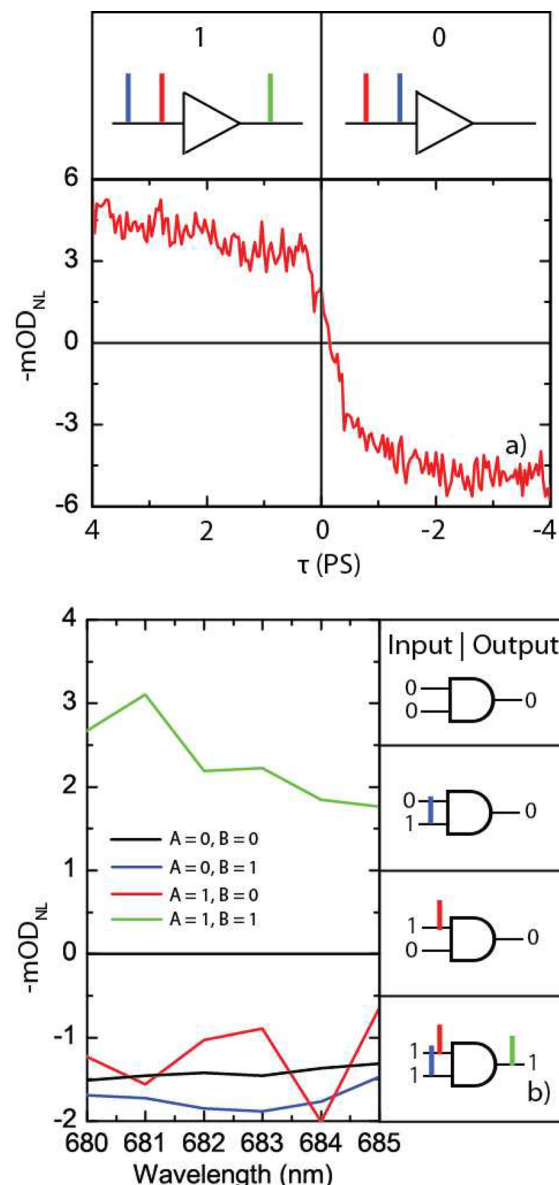


Figure 4. (a) The modulator arrival time is swept from $\tau = 4$ ps to -4 ps to determine pump-ordering dependence corresponding to an ON-OFF bit pattern with $T = 6$ ps. The switching transient shows an ON-OFF (stimulated emission/absorption) response due to time encoding of the pulses in an inverter scheme. Saturator and modulator pulses are depicted as red and blue, respectively, with the output (green) being the presence or absence of stimulated emission (top). (b) Logic table and output of all-optical AND gate. Inputs were fixed to $T = 3$ ps, $\tau = 1$ ps and altered via optical chopping. Stimulated emission, denoted by $-\text{mOD}_{\text{NL}} > 0$, occurred only in the event of both optical inputs. For logic table, saturator and modulator pulses are depicted as red and blue, respectively, with the output (green) being the presence or absence of stimulated emission.

prepared by the modulator pulse creates the signal on top of the background from the SE_{XX} created by the saturator pulse. This decomposition of SE into contributions from specific multie excitons rationalizes the contrast ratio of the switch. Because of spectral overlap between MX states,¹⁶ contrast is diminished. This contrast can be improved by increasing MX interaction strengths or decreasing the SE linewidths.

The modulation bandwidth is dictated by the MX recombination rates that correspond to the ON and OFF

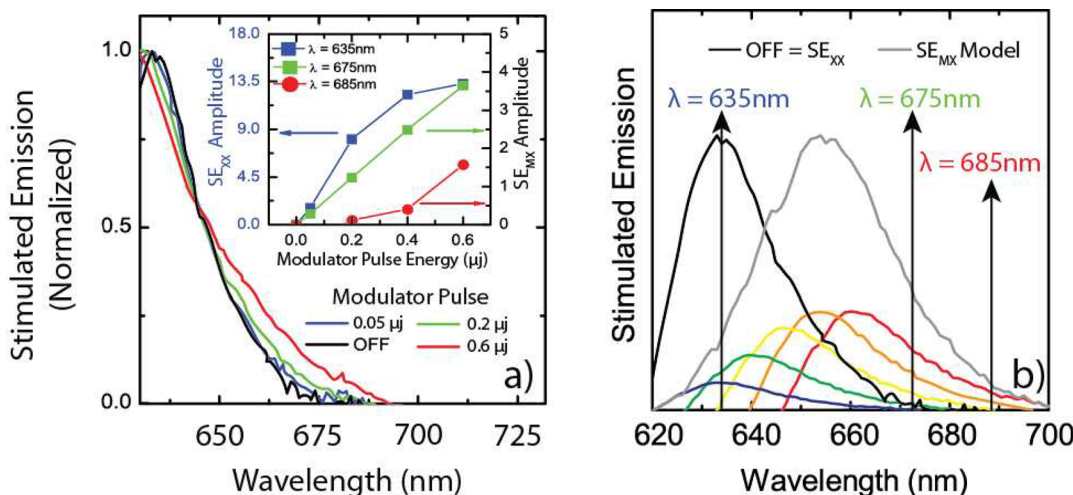


Figure 5. (a) Fluence dependence of SE modulation amplitude with $\tau = 2$ ps and $T = 4$ ps. The inset shows the wavelength dependence, revealing increasing nonlinearity due to higher multiexcitons. (b) The modulation channels as well as the contrast ratios are dictated by the MX spectra. The saturator produces SE_{XX} (OFF) whereas the modulator produces a Poisson distribution of MX which sums to SE_{MX} .

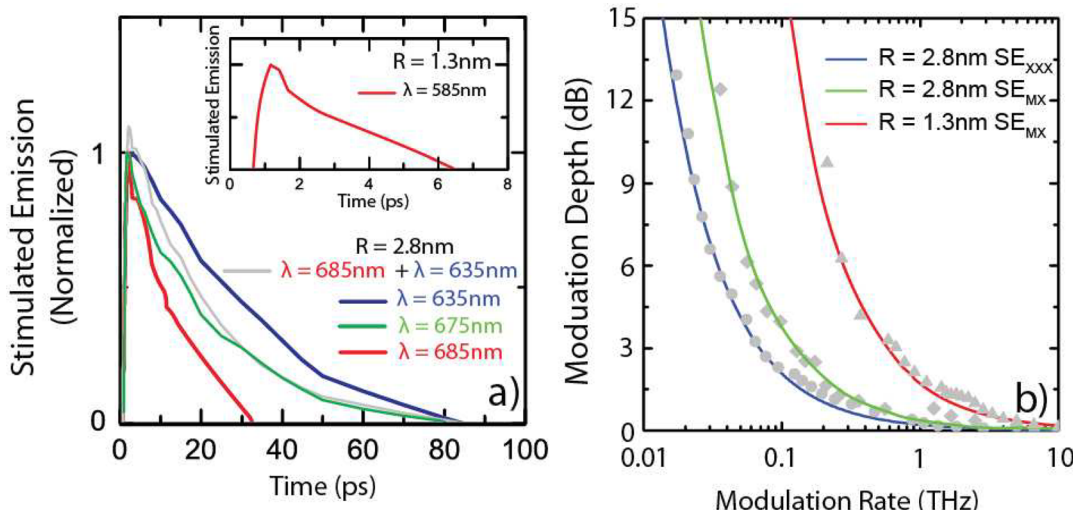


Figure 6. (a) The modulation rate is dictated by the MX recombination rates. The transient at 635 nm corresponds to XX state, whereas the transient at 685 nm corresponds to higher MX. The intermediate 675 nm transient is well described as a sum of XX and MX transients due to spectral overlap. The inset shows a faster response for smaller NC ($R = 1.3$ nm). (b) Modulation spectra can be controlled by both NC size and MX multiplicity. The colored curves correspond to a simulation, and the gray points correspond to contrast ratios obtained from the experimental SE transients.

213 states. To directly determine these rates, we measure the SE
214 lifetimes of the XX as well as higher MX states, Figure 6a. At
215 longer wavelengths, the SE curves decay faster. This response is
216 anticipated from knowledge of the quantized Auger recombi-
217 nation rates of multiexcitons in these nanocrystals.¹⁵ We show
218 the SE curves for $R = 2.8$ nm CdSe/ZnS at three wavelengths
219 and $R = 1.3$ nm CdSe/ZnS at one wavelength. Probing at 635
220 nm demonstrates SE decay in agreement with the XX lifetime
221 and the SE at 685 nm decays more rapidly, consistent with
222 higher MX multiplicity. The noteworthy point is that the 675
223 nm SE transient is perfectly reproduced as a sum of 635 and
224 685 nm transients, corresponding to the signal arising as a sum
225 of XX and higher MX contributions, as shown in Figure 5b. As
226 expected, the smaller nanocrystal has a faster recovery time,
227 enabling higher modulation bandwidths.

228 We analyze this switch by modeling as well as directly from
229 the data, Figure 6b. The modulation spectrum is dictated by the
230 lifetimes of the multiexcitonic states¹⁵ and also the spectral

overlap between the SE signals from the XX and MX states.^{14,16} Upon the basis of published recombination rates and the MX spectral decomposition above, we simulate the switching spectrum. In addition, the SE data was directly analyzed to extract the time dependent contrast ratios that determine the switch spectrum. Both are shown in Figure 6b with near perfect agreement. This analysis shows that higher multiexcitons enable faster switching as does smaller nanocrystals. Notably, the 3 dB modulation bandwidths can approach 1 THz.

In summary, we have demonstrated that multiexcitons in semiconductor nanocrystals can form the basis of ultrafast all optical switching at terahertz rates. Upon the basis of dual inputs and time ordering, this approach has enabled realization of Boolean logic with an AND gate as well as signal inversion. The mechanism driving the modulation rate is multiexcitonic (Auger) recombination. This room temperature AND gating is made possible by the large interaction energies unique to these NC. This work reveals a completely new mechanism by which

249 optical signals may be modulated, as well as a new area of
250 impact for semiconductor nanocrystals.

(24) Cooney, R. R.; Sewall, S. L.; Dias, E. A.; Sagar, D. M.; Anderson, 310
K. E. H.; Kambhampati, P. *Phys. Rev. B* 2007, 75 (24), 245311–14. 311

251 ■ ASSOCIATED CONTENT

252 ■ Supporting Information

253 Additional information and figures. This material is available
254 free of charge via the Internet at <http://pubs.acs.org>.

255 ■ AUTHOR INFORMATION

256 Corresponding Author

257 *E-mail: Pat.Kambhampati@mcgill.ca.

258 Notes

259 The authors declare no competing financial interest.

260 ■ ACKNOWLEDGMENTS

261 Financial support from CFI, NSERC, FQRNT is acknowl-
262 edged. The authors thank Thomas Szkopek for helpful
263 discussions. The authors would also like to thank Samuel
264 Sewall for assistance.

265 ■ REFERENCES

- 266 (1) Miller, D. A. B. *Nat. Photonics* 2010, 4 (1), 3–5.
267 (2) Gur, I.; Fromer Neil, A.; Geier Michael, L.; Alivisatos, A. P.
268 *Science* 2005, 310 (5747), 462–5.
269 (3) Huynh Wendy, U.; Dittmer Janke, J.; Alivisatos, A. P. *Science*
270 2002, 295 (5564), 2425–7.
271 (4) Klimov, V. I.; Ivanov, S. A.; Nanda, J.; Achermann, M.; Bezel, I.;
272 McGuire, J. A.; Piryatinski, A. *Nature* 2007, 447 (7143), 441–446.
273 (5) Klimov, V. I.; Mikhailovsky, A. A.; Xu, S.; Malko, A.;
274 Hollingsworth, J. A.; Leatherdale, C. A.; Eisler, H. J.; Bawendi, M.
275 G. *Science* 2000, 290 (5490), 314–317.
276 (6) Konstantatos, G.; Sargent, E. H. *Nat Nanotechnol.* 2010, 5 (6),
277 391–400.
278 (7) Coe, S.; Woo, W.-K.; Bawendi, M.; Bulovic, V. *Nature* 2002, 420
279 (6917), 800–803.
280 (8) Kambhampati, P. *Acc. Chem. Res.* 2011, 44 (1), 1–13.
281 (9) Kambhampati, P. *J. Phys. Chem. C* 2011, 115 (45), 22089–22109.
282 (10) Klimov, V. I. *Annu. Rev. Phys. Chem.* 2007, 58, 635–673.
283 (11) Efros, A. L.; Rosen, M. *Annu. Rev. Mater. Sci.* 2000, 30, 475–
284 521.
285 (12) Norris, D. J.; Bawendi, M. G. *Phys. Rev. B* 1996, 53 (24),
286 16338–16346.
287 (13) Cooney, R. R.; Sewall, S. L.; Sagar, D. M.; Kambhampati, P.
288 *Phys. Rev. Lett.* 2009, 102 (12), 127404–4.
289 (14) Cooney, R. R.; Sewall, S. L.; Sagar, D. M.; Kambhampati, P. *J.*
290 *Chem. Phys.* 2009, 131, 164706.
291 (15) Klimov, V. I.; Mikhailovsky, A. A.; McBranch, D. W.;
292 Leatherdale, C. A.; Bawendi, M. G. *Science* 2000, 287 (5455),
293 1011–1013.
294 (16) Sewall, S. L.; Cooney, R. R.; Dias, E. A.; Tyagi, P.;
295 Kambhampati, P. *Phys. Rev. B* 2011, 84 (23), 235304.
296 (17) Fisher, B.; Caruge, J. M.; Chan, Y. T.; Halpert, J.; Bawendi, M.
297 G. *Chem. Phys.* 2005, 318 (1–2), 71–81.
298 (18) Osovsky, R.; Cheskis, D.; Kloper, V.; Sashchiuk, A.; Kroner, M.;
299 Lifshitz, E. *Phys. Rev. Lett.* 2009, 102 (19), 197401–4.
300 (19) Sewall, S. L.; Cooney, R. R.; Anderson, K. E. H.; Dias, E. A.;
301 Kambhampati, P. *Phys. Rev. B* 2006, 74 (23), 235328.
302 (20) Cooney, R. R.; Sewall, S. L.; Anderson, K. E. H.; Dias, E. A.;
303 Kambhampati, P. *Phys. Rev. Lett.* 2007, 98 (17), 177403–4.
304 (21) Sewall, S. L.; Cooney, R. R.; Anderson, K. E. H.; Dias, E. A.;
305 Sagar, D. M.; Kambhampati, P. *J. Chem. Phys.* 2008, 129 (8), 084701.
306 (22) Sewall, S. L.; Franceschetti, A.; Cooney, R. R.; Zunger, A.;
307 Kambhampati, P. *Phys. Rev. B* 2009, 80 (8), 081310(R).
308 (23) Sewall, S. L.; Cooney, R. R.; Kambhampati, P. *Appl. Phys. Lett.*
309 2009, 94 (24), 243116–3.